Fundamentals of electron energy-loss spectroscopy

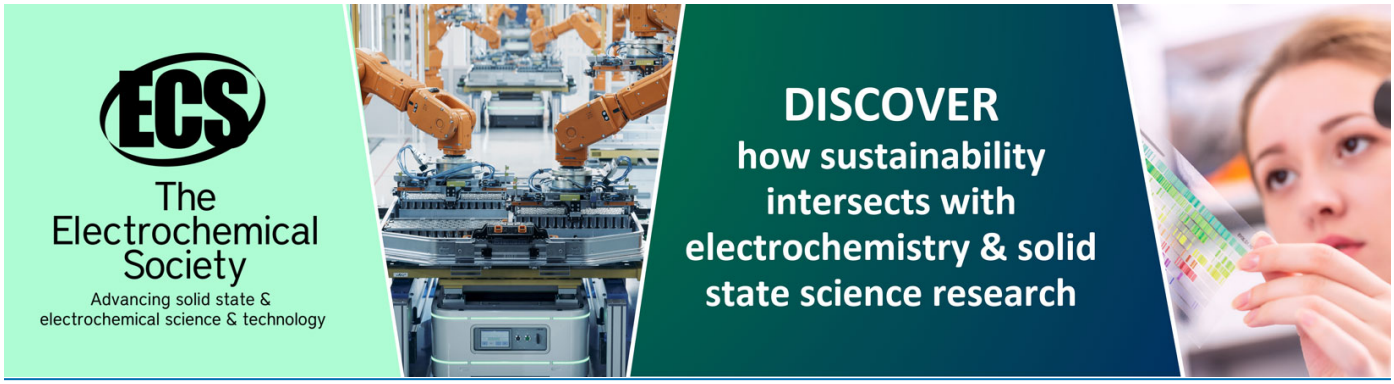

IOP Conf. Series: Materials Science and Engineering **109** (2016) 012007 doi:10.1088/1757-899X/109/1/012007

Fundamentals of electron energy-loss spectroscopy

F Hofer, F P Schmidt, W Grogger and G Kothleitner

Graz University of Technology and Graz Centre for Electron Microscopy, Institute of Electron Microscopy and Nanoanalysis, Steyrergasse 17, 8010 Graz, Austria

E-mail: ferdinand.hofer@tugraz.at

Abstract. Electron energy-loss spectroscopy (EELS) is an analytical technique that is based on inelastic scattering of fast electrons in a thin specimen. In a transmission electron microscope (TEM) it can provide structural and chemical information about a specimen, even down to atomic resolution. This review provides an overview of the physical basis and new developments and applications of EELS in scanning transmission electron microscopy. Recent advances in elemental mapping, spectrum imaging of plasmonic structures and quantitative analysis of atomically resolved elemental maps are highlighted.

1. Introduction

The need to understand atomic processes in solids has led to an increasing demand for new imaging, diffraction and spectroscopy methods with high spatial resolution. This need has been reinforced by the growing interest in nanoscience and nanotechnology. Particularly, transmission electron microscopy (TEM) is of unrivalled value, because it can provide structural information with excellent spatial resolution (down to atomic dimensions) via high resolution TEM imaging and electron diffraction. These structural data can be supplemented by chemical information from the same specimen region, obtained using analytical techniques, such as energy-dispersive X-ray spectroscopy (EDS) and electron energy-loss spectroscopy (EELS) [1].

Due to the broad range of inelastic interactions of the high energy electrons with the specimen atoms, ranging from phonon interactions to ionisation processes, electron energy-loss spectroscopy offers unique possibilities for advanced materials analysis. It can be used to map the elemental composition of a specimen, but also for studying the physical and chemical properties of a wide range of materials and biological matter.

Beginning with the increasing use of EEL spectrometers during the eighties of the last century [1], the energy-filtering technique was a major step forward for two-dimensional mapping of the spectral features visible in an EEL spectrum [2, 3]. The wide distribution of energy-filtering TEMs (EFTEM) led to numerous practical applications both in the materials and biological sciences [4]. In the meanwhile, EFTEM is a widely used method for both overview and nanoscale characterisation of thin samples, applicable to most chemical elements and especially sensitive to light elements.

With the introduction of high brightness electron sources and spherical aberration correctors, the image resolution of the TEM reaches now the 50 picometre level [5]. Especially scanning transmission electron microscopy (STEM) equipped with a Cs-probe corrector is extremely useful for high resolution imaging [6] and the parallel chemical analysis by EELS and EDS because of the much increased probe current in the corrected beam.

Before discussing how these various methods and their recent developments provide us with information about the specimen, we will briefly examine the principles and instrumentation involved in recording energy-loss spectra in the TEM.

2. The electron energy-loss spectrum

A beam electron in a (S)TEM may be inelastically scattered when it interacts with the atomic electrons in the specimen. The electron beam loses energy and is bent through a small angle (5 - 100 milliradians). The energy distribution of all the inelastically scattered electrons provides information about the local environment of the atomic electrons which in turn relates to the physical and chemical properties of the specimen. This is the basis of electron energy-loss spectroscopy (EELS) [1]. Much of the information obtainable from EELS is similar to that of X-ray absorption spectrometry (XAS) in the synchrotron.

Figure 1 shows a typical electron energy-loss spectrum recorded up to 600 electron volts. The first peak, the most intense for a very thin specimen, occurs at 0 eV and is therefore called the zero-loss peak. It represents electrons which have not been scattered in the specimen (transmitted electrons) and which have been elastically scattered via interaction with the atomic nuclei.

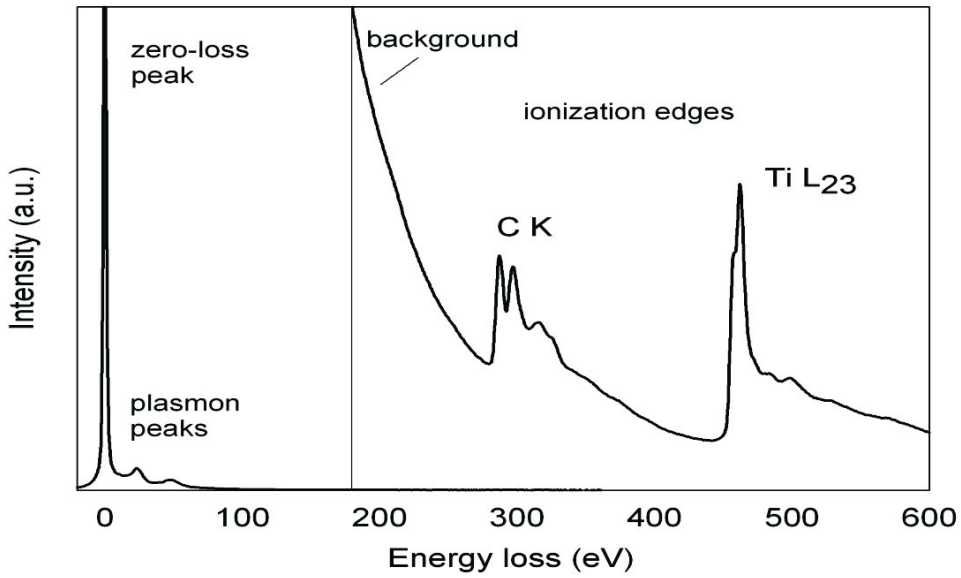

Figure 1. EELS spectrum of a 20 nm thin titanium carbide specimen recorded in a conventional 200 kV TEM equipped with an energy-filtering spectrometer.

The low-loss or valence region of an EEL spectrum (< 50 eV) provides similar information to that provided by optical spectroscopy, containing valuable information about the band structure and in particular about the dielectric properties of a material (e.g., band gap, surface plasmons). The most prominent peak, centred at 24 eV, comes from a plasma resonance of the valence atoms. Signal intensities in the low-loss region are larger than in the high-loss region of the spectrum.

At higher energy losses (> 50 eV), where the number of inelastically scattered electrons is much lower, the spectrum shows characteristic features called “ionisation edges” (due to their typical shape, a rapid rise followed by a more gradual fall). These edges are the exact equivalent of an absorption edge in XAS and arise from the same process. The edges are formed when an inner-shell electron absorbs enough energy from a beam electron to be excited to a state above the Fermi level. Not all ionisation edges are saw-toothed like the carbon K-edge in figure 1, but exhibit more complex edge

shapes such as the $L_{2,3}$-edge of titanium in figure 1. This $L_{2,3}$-edge includes sharp excitations at the onset of the ionisation edge, called white-lines, which are typical for elements in the first row of transition elements and for the rare earth elements. The ionisation edges can be used for the analysis of almost all chemical elements in particular for the lighter elements, the edge onset gives the ionisation energy and allows the qualitative analysis and in case of very thin samples the edge intensities are proportional to the concentration of the corresponding elements.

3. Recent advances in EELS methodology

TEM-EELS instrumentation is based on a magnetic prism, in which a uniform magnetic field is generated by an electromagnet with specially designed pole pieces. The prism bends the inelastically scattered electrons by about 90^{o}, disperses them according to their different kinetic energies and also has a focussing action. The spectra are recorded with a charge coupled device (CCD camera). Due to the enormous dynamic range of an EEL spectrum, spanning many orders of magnitude, and due to restrictions in dynamic range and sensitivity of CCD based spectrometers, a complete EEL spectrum normally has to be recorded in several segments by changing illumination conditions and/or acquisition times.

Energy filters are used to form images from electrons that have suffered a specific energy loss [energy filtered TEM (EFTEM) or electron specific imaging (ESI)]. In particular, two types of energy-filtering instruments are most often used: firstly post-column energy filters, with a single prism geometry and multipole lenses, can be attached and retrofitted to practically any TEM or STEM instrument [7]. The post-column filter is not only an efficient imaging system, but also a versatile instrument for acquiring EEL spectra in high quality. Secondly the in-column filter, whose spectrometer consists of four magnetic prisms that are arranged symmetrically according to the shape of a Greek Omega, is located below the projector lens system of the TEM. This type of filter can be also used for spectroscopy, but the main application field is high quality imaging such as large area elemental mapping and energy-filtered electron diffraction studies [8].

Another important development was the introduction of monochromators for the electron source, which paved the way for acquiring EEL spectra at high energy resolution, typically in the 100 - 200 meV range (e.g., the Wien filter approach) [9]. The improved energy resolution opens new possibilities for studying detailed electronic structure and bonding effects evaluated from near edge fine structures of the ionisation edges, but also accurate band gap and dielectric function measurements via the low-loss part of the spectrum [1].

Several years ago, the problem of the high dynamic range of the EEL spectrum could be addressed by acquiring the elastic and inelastic parts at nearly coincident times at identical experimental conditions, offering the advantage of using the low-loss regime as a reference for quantitative data analysis. This system works with an additional electrostatic vertical deflector and is now successfully used by several groups worldwide [10, 11].

Advances in X-ray detection with the advent of large area or four-quadrant solid state silicon drift detectors [12] and the rapid progress in EDS data processing, pushed the ideas for highly efficient elemental mapping in combination with EELS. The collaboration between Gatan, Bruker and the TU Graz enabled the fast recording of multimodal data so that STEM-images, low-loss and high-loss EELS and EDS data can now be acquired with a speed of 1,000 to 1,500 spectra per second [13].

While the conventional method of EELS mapping combines TEM/STEM images with the local concentration of the elements, the development of more powerful computers and data reduction procedures nowadays allows a “holistic” approach: the whole spectral information is gathered for each point of an image, generating a three-dimensional data set which is often called a spectrum image [14]. The spectrum-imaging technique offers various advantages: the wealth of data allows a certain amount of “post experiment microscopy” and because of the completeness of data, interpretation mistakes can be avoided. Additionally, a data-evaluation software can automatically identify and highlight the most prominent features, e.g., chemical phases [15]. Therefore, spectrum-imaging techniques are the essential basis for successful EELS mapping at the atomic scale.

4. Elemental mapping at high spatial resolution

One of the most commonly used applications of STEM-EELS or EFTEM is to derive compositional information by recording energy-filtered images using the element characteristic ionisation edges. Although advanced energy-filters or spectrometers now enable the fast acquisition of elemental maps almost on a routine basis, care must be taken due to several experimental limitations of EELS: generally, the signal-to-noise ratio of the elemental signal is very low which is mainly caused by the high uncharacteristic background below the ionisation edges and the low ionisation cross-sections for heavier elements and for elements occurring at low concentrations.

Another important limitation comes from multiple scattering of the inelastic signal in thicker specimens, restricting elemental mapping to specimen thicknesses well below the mean free path lengths of the inelastically scattered electrons (specimen thickness < 70 nm for most materials). Alternatively, EELS spectra from thicker specimens may be deconvolved by using the low-loss part of the EELS spectrum, recovering a single scattering distribution EELS spectrum. Typical procedures involve Richardson-Lucy or Fourier log methods [16, 17], which however decrease the signal-to-noise ratio of the spectrum. When crystalline specimens are studied, a frequent problem is the preservation of diffraction contrast in inelastic imaging, which can be reduced by employing advanced illumination conditions (hollow-cone or rocking-beam illumination) [2].

Firstly, detailed strategies had to be developed to optimize the quality of the experimental spectrum. Secondly, advanced spectrum imaging techniques, which include a variety of data correction or processing procedures, are a prerequisite for successful elemental mapping with EELS or EFTEM [15, 18] (see example in figure 2). Additionally, it is known for a long time that EELS spectra or elemental maps can be quantified using the standard EELS quantification procedures thus providing absolute and relative concentration values at the nanometre scale [1, 19].

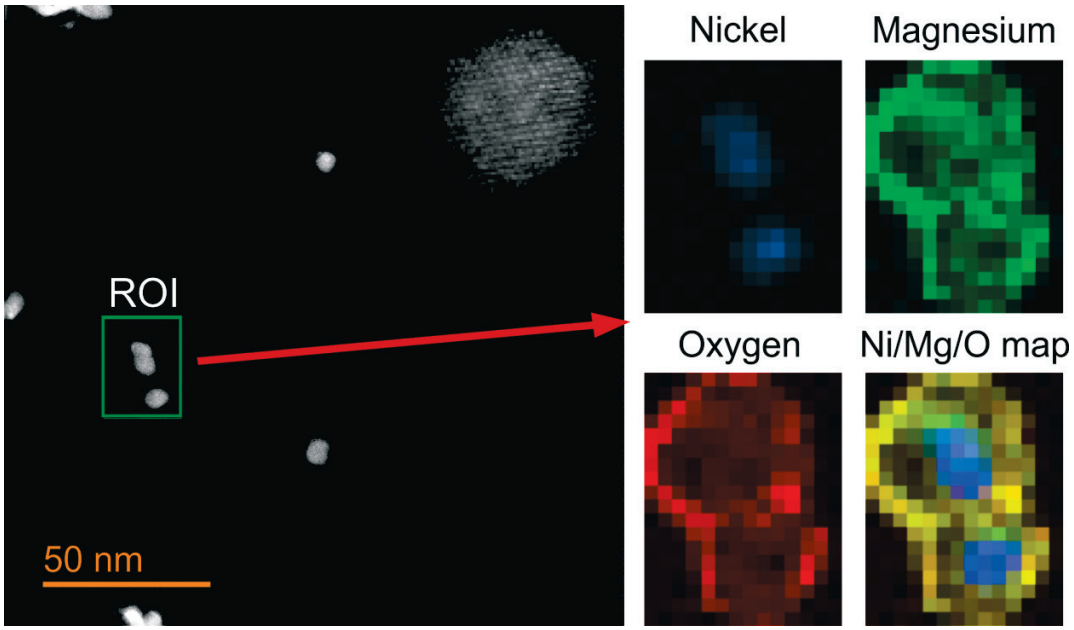

Figure 2. MgO/Ni core shell nanoparticles investigated with a C_S-corrected STEM and EELS spectrum imaging revealing the Ni core and the MgO shell, the inset shows the Z-contrast image of the Ni core (specimen courtesy: Gopi Krishnan, University of Groningen, The Netherlands).

Although EFTEM elemental mapping is now widely used for nanoscale analysis, it cannot deliver atomic resolution information even in aberration-corrected TEMs. Since the C_S-image corrector affects only spherical aberrations, but not chromatic aberrations (C_C), EFTEM mapping at atomic resolution is only possible by incorporating a chromatic aberration corrector. This so far is only realized at the NCEM in Berkeley (USA) and the Ernst-Ruska Center in Jülich (Germany) [20].

Elemental mapping at atomic resolution can be easier achieved via the scanning transmission electron microscope (STEM) which is now in wide general use, harnessing Z-contrast imaging and EELS [21]. The first elemental maps at atomic resolution have been recorded by using the STEM-EELS technique by Kimoto *et al.* [22] and they have been able to visualize the atomic columns of La, Mn and O in the layered manganite $La_{1.2}Sr_{1.8}Mn_2O_7$. In the meanwhile Allen and co-workers [23] have shown that it is also possible to record atomically resolved elemental maps by using X-ray spectroscopy in the STEM.

Two important developments enhanced the potential for successful elemental mapping at atomic resolution: Firstly, the introduction of collection-efficient solid state X-ray detectors (SDD) [12] and secondly, the simultaneous acquisition of EELS and EDS spectrum images with fast scanning rates [13]. Since then many examples of atomically resolved elemental maps have been published, but it has to be realized that coloured elemental maps only yield qualitative information. However, it is extremely important to provide quantification data in terms of volumetric densities (i.e., number of atoms per unit volume), as it allows correlating structural and chemical information with each other ("unit cell atom counting"). Using a $SrTiO_3$ crystal of known thickness and density Kothleitner *et al.* [24] could show how EELS and EDS elemental maps (figure 3) can be quantified by combining both spectroscopies and including the zeta factor method for X-ray quantification. The results show that it is possible to obtain quantitative numbers of Sr, Ti and O atoms in the individual atom columns, however elastic and thermal scattering effects can severely influence accuracy at atomic resolution [25].

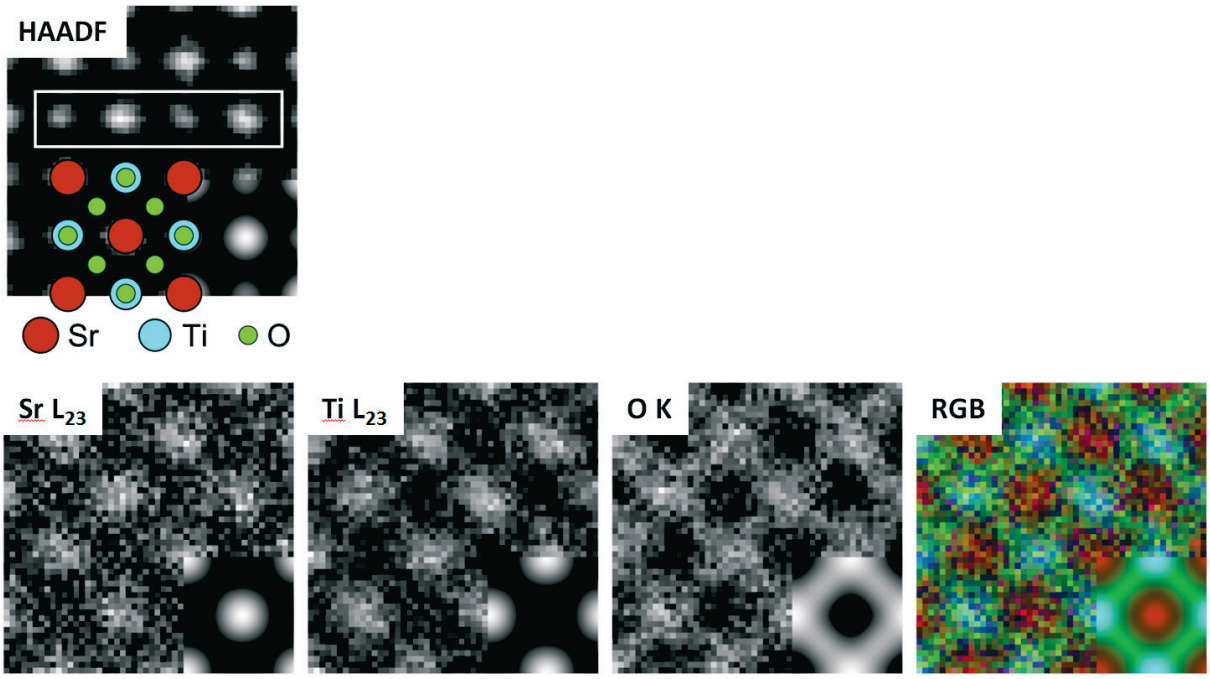

Figure 3. Experimental atomic resolution EELS elemental maps for the {001} direction in $SrTiO_3$ for the Sr $L_{2,3}$-edge, the Ti $L_{2,3}$- and the O K-edge with the simultaneously acquired HAADF image and the RGB composite of the elemental maps; quantum mechanical simulations, assuming a Gaussian incoherent source size of 0.08 nm, are inset in each figure; from [25].

5. Chemical bonding information

Edge fine structures arouse considerable interest in the application of EELS, especially in the field of materials science, because they can be used to extract information regarding local charge distributions, coordination numbers and bonding characteristics. The fine structures are divided into the near edge-fine structures (ELNES) within 50 eV of the edge onset and the extended fine structure (EXELFS) about some 100 eV above the edge onset. Most of the ionisation edges contain a more complex structure than can be explained in simple atomic terms. The ionisation edges are often modified by the solid state environment of the atom undergoing the inner-shell excitation and this information can be used as a "fingerprint" from elements in similar chemical environments [26, 27]. In the meanwhile the calculation of ELNES structures has reached a high degree of sophistication [28].

One important development for ELNES studies was the introduction of the monochromated (S)TEMs which helped to improve the instrumental energy resolution to values as low as 100 meV. In combination with advanced energy-filters and/or spectrometers it was now possible to fully exploit informational the spectral details contained in the EEL spectrum. It was not at all obvious, however, at the time of the development during the late nineties that these tools would gain such importance. The reduced energy spread of the TEM immediately opened possibilities for detailed studies of the near-edge fine structures at K- and $L_{2,3}$-ionisation edges of oxides, perovskites and similar materials [29]. The knowledge about these ELNES structures at high energy resolution is an important basis for STEM-EELS imaging of chemical bonding in materials. Figure 4 shows the ELNES structure of the V $L_{2,3}$ white lines of V_2O_5 recorded at different energy resolutions. The L_3 white line reveals the symmetry of the vanadium site being surrounded by six oxygen atoms forming a strongly distorted octahedron unit [30].

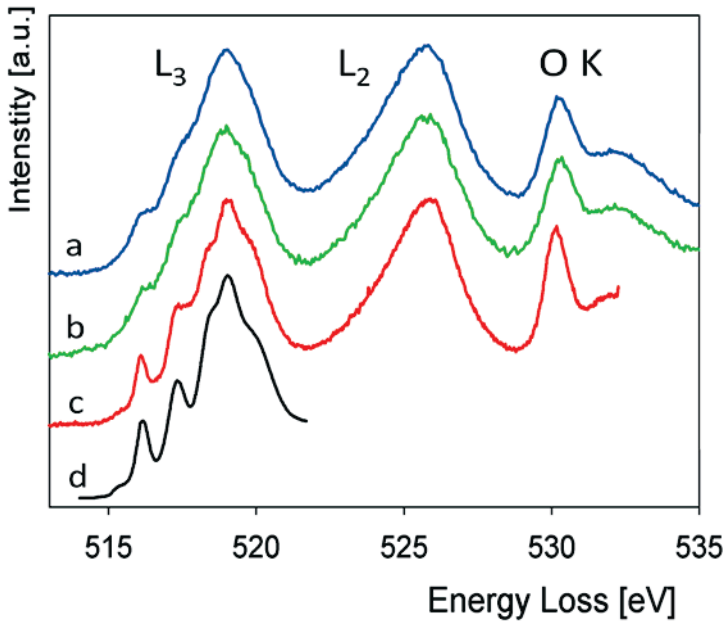

Figure 4. Comparison of the V $L_{2,3}$- and O-ionisation edges of V_2O_5 which have been recorded with different energy resolution; a) 200 kV TEM with LaB_6 cathode (0.7 eV); b) 200 kV TEM with Schottky emitter (0.6 eV); c) 200 kV TEM with a monochromator and a HR-energy-filter (0.3 eV); d) X-ray absorption spectrum recorded with an energy resolution of 0.08 eV; from [30].

6. Physical property mapping

The low-loss spectrum contains energy losses to valence or conduction electrons which provide rich information about the physical properties of a specimen e.g., inter- or intraband transitions, band gaps and the dielectric properties [31, 32]. One important application of low-loss EELS lies in the study of optical properties of metallic nanostructures which may drastically change at the nanometre scale as a function of size, morphology and environment. In particular, collective oscillations of quasi free

electrons on a metallic/dielectric interface, i.e., surface plasmons, are increasingly studied in the (S)TEM, taking advantage of its unbeaten high spatial resolution (compared to the scanning optical near-field microscope). Here the introduction of monochromators, providing an energy resolution of 100 meV or even less [33], was mainly responsible for the big success of the technique [34].

Since the early seventies of the last century EELS has been used for studying surface plasmons [31, 35], but it was only in 2007 when two independent groups showed how fast electrons can be used to map localized surface plasmons of single noble metal nanoparticles [36, 37]. In these pioneering works STEM-EELS was used, but later it was also shown that a monochromated EFTEM can yield comparable results [38, 39]. It is now widely accepted that EELS or EFTEM are the most advanced methods to probe plasmonic modes and they are increasingly used to study nanostructures of increasing complexity. For example STEM-EELS was used for studying dark plasmonic breathing modes in silver nanodisks [40], for morphing a plasmonic nanodisk into a nanotriangle [41], for revealing universal dispersions of surface plasmons in flat nanostructures [42], for studying the 3D distribution of surface plasmons around a metal nanoparticle [43] and for exotic nanostructures as shown in figure 5.

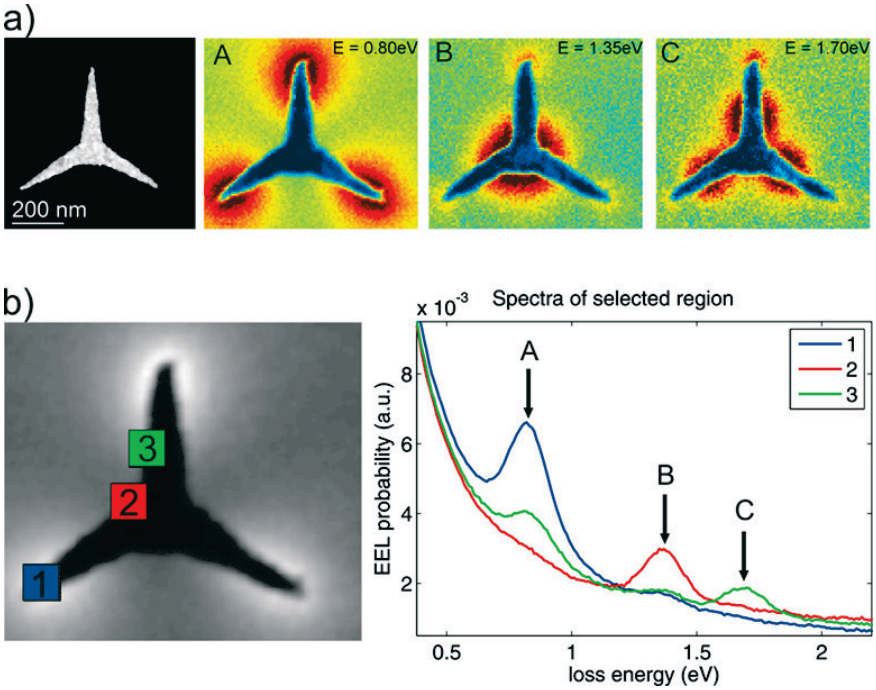

Figure 5. a) High-angle annular dark field (HAADF) image of a 30 nm thick Au-nanostar on a 15 nm thin silicon nitride membrane (left) and corresponding electron energy loss (EEL) maps at 0.8 eV (A), 1.35 eV (B) and 1.70 eV (C) integrated over an energy width of 150 meV. The EELS maps were generated using the STEM-EELS approach with a monochromated 200 keV electron beam with 150 meV energy resolution (FWHM). The sample was prepared by electron beam lithography, raw data are presented. B) The regions 1-3 in the spectrum image (left) mark the areas from which EEL spectra were extracted. The peaks labelled by A, B and C corresponds to the energies of the EELS maps shown in (a).

Recent progress in the development of monochromators with improved energy resolution in the range of 10 meV has shown that it is now possible to reveal vibrational modes (phonons) in EEL spectra recorded in a STEM [44]. This new technique allows to study the spatial variation of vibrational modes in nanostructures and nanoparticles.

7. Conclusions

Overall, inelastic excitations, probed by electron microscopy, have been a continuous source of information on composition, chemical and physical properties of nanostructured materials over the last decades. In this review we briefly describe the physical basis of electron energy-loss spectroscopy and recent developments in EELS instrumentation. We show how STEM-EELS can be used for elemental mapping of heterogeneous nanoparticles and discuss the prospects for quantitative elemental analysis at atomic resolution. We describe the advantages of monochromated STEMs for obtaining chemical bonding information from the EELS near-edge fine structures. Furthermore, we explain how the low-loss region of the EEL spectrum can be used for physical property mapping. Here we concentrate on surface plasmon imaging of noble metal nanoparticles. In summary, EELS imaging and spectroscopy with aberration corrected STEMs offer many new opportunities to study fundamental questions in physics, chemistry and materials science at atomic resolution.

Acknowledgements

This work has received funding from the European Union within the 7th Framework Programme under Grant Agreement no. 312483 (ESTEEM2). This work was financially supported by the FFG in Vienna, Austria (COIN-project ASTEM).

References

[1] Egerton R F 2011 *Electron energy-loss spectroscopy in the electron microscope, 3rd edition*. (New York-Dordrecht-Heidelberg-London: Springer)
[2] Shuman H, Chang C F and Somlyo A P 1986 *Ultramicroscopy* **19** 121
[3] Mayer J 1992 in: *Proc. 50th EMSA Meeting.* (San Francisco, CA: San Francisco Press) 1198-1199
[4] Hofer F and Warbichler P 2004 in: *Transmission electron energy loss spectrometry in materials science and the EELS atlas. 2nd edition.* (Ahn C C; Ed.) (Weinheim: Wiley-VCH) 159-222
[5] Haider M, Uhlemann S., Schwan E, Kabius B and Urban K 1998 *Nature* **392** 768
[6] Batson P E, Dellby N and Krivanek O L 2002 *Nature* **418** 617
[7] Krivanek O L, Gubbens A J, Dellby N and Meyer C E 1991 *Microsc. Microanal. Microstruct.* **2** 315
[8] Mayer J, Deininger C and Reimer L 1995 in: *Energy-filtering transmission electron microscopy*. (Reimer L; Ed.) (Berlin-Heidelberg-New York: Springer Verlag) 291-346
[9] Tiemeijer P C 1999 *J. Phys.: Conf. Ser.* **161** 191-194
[10] Scott J, Thomas P J, MacKenzie M, McFadzean S, Wilbrink J, Craven A J and Nicholson W A P 2008 *Ultramicroscopy* **108** 1586
[11] Angseryd J, Albu M, Andren H O and Kothleitner G 2011 *Micron* **42** 608
[12] Von Harrach H S, Dona P, Freitag B, Soltau H, Niculae A and Rohde M 2010 *J. Phys.: Conf. Ser.* **241** 012015
[13] Kothleitner G, Fladischer S, Grogger W, Haber T, Meingast A and Hofer F 2012 *Microsc. Microanal.* **18** (Suppl. 2) 972
[14] Jeanguillaume C and Colliex C 1989 *Ultramicroscopy* **28** 252
[15] Schaffer B, Kothleitner G and Grogger W 2004 *Ultramicroscopy* **106** 1129
[16] Gloter A, Douiri, Tence M. Colliex C 2003 *Ultramicroscopy* **96** 385
[17] Thomas P J and Midgley P A 2001 *Ultramicroscopy* **88** 187
[18] Kothleitner G and Hofer F 1998 *Micron* **29** 349

[19] Hofer F, Grogger W, Kothleitner G and Warbichler P 1997 *Ultramicroscopy* **67** 83
[20] Urban K W, Mayer J, Jinschek J R, Neish M J, Lugg N R and Allen L J 2013 *Phys. Rev. Lett.* **110** 185507
[21] Pennycook S J and Nellist P D 2011 *Scanning transmission electron microscopy.* (New York-Dordrecht-Heidelberg-London: Springer)
[22] Kimoto K, Asaka T, Nagai T, Saito M, Matsui Y and Ishizuka 2007 *Nature* **450** 702
[23] Allen L J, D'Alfonso A J, Freitag B. and Klenov D O 2012 *MRS Bull.* **37** 47
[24] Kothleitner G *et al.* 2014 *Microsc. Microanal.* **20** 678
[25] Kothleitner G, Neish M J, Lugg N R, Findlay S D, Grogger W, Hofer F and Allen L J 2014 *Phys. Rev. Lett.* **112** 085501
[26] Hofer F and Golob P 1987 *Ultramicroscopy* **21** 379
[27] Keast V J, Scott A J, Brydson R, Williams D B and Bruley J 2001 *J. Microscopy* **203** 135
[28] Rez P, Alvarez J R and Pickard C 1999 *Ultramicroscopy* **78** 175
[29] Mitterbauer C, Kothleitner G, Grogger W, Zandbergen H, Freitag B, Tiemeijer P and Hofer F 2003 *Ultramicroscopy* **96** 469
[30] Su D S, Zandbergen H W, Tiemeijer P C, Kothleitner G., Hävecker M, Hebert C, Knop-Gericke A, Freitag B H, Hofer F and Schlögl R 2003 *Micron* **34** 235
[31] Geiger J 1967 *Phys. Stat. Sol.* **24** 457
[32] Schattschneider P 1986 *Fundamentals of inelastic electron scattering.* (Vienna, Austria: Springer)
[33] Schaffer B, Riegler K, Kothleitner G, Grogger W and Hofer F 2009 *Micron* **40** 269
[34] Grogger W, Hofer F, Kothleitner G and Schaffer B 2008 *Top. Catal.* **50** 200
[35] Batson P E 1980 *Solid State Comm.* **34** 477
[36] Nelayah J, Kociak M, Stephan O, de Abajo G, Javier F, Tence, Henrard L, Taverna D, Pastoriza-Santos, Liz-Marzan L M and Colliex C 2007 *Nature Phys.* **3** 348
[37] Bosman M, Keast V J, Watanabe M, Maarof A I and Cortie M B 2007 *Nanotechnology* **18** 165505
[38] Schaffer B, Hohenester U, Trügler A and Hofer F 2009 *Phys. Rev. B* **79** 041401
[39] Schaffer B, Grogger W, Kothleitner G and Hofer F 2010 *Ultramicroscopy* **110** 1087
[40] Schmidt F P, Ditlbacher H, Hohenester U, Hohenau A, Hofer, F and Krenn J R 2012 *Nano Lett.* **14** 5780
[41] Schmidt F P, Ditlbacher H, Hofer F, Krenn J R and Hohenester U 2014 *Nano Lett.* **14** 4810
[42] Schmidt F P, Ditlbacher H, Hohenester U, Hohenau A, Hofer F and Krenn J R 2014 *Nature Comm.* **5** 3604
[43] Nicoletti O, de la Peña F, Leary R K, Holland D J, Ducati C, Midgley P A 2013 *Nature* **502** 80
[44] Krivanek O L, Lovejoy T C, Dellby N, Aoki T, Carpenter R W, Rez P, Soignard E, Zhu J, Batson P E, Lagos M J, Egerton R F and Crozier P A 2014 *Nature* **514** 209